Robust Use of Horizontal Stabilator in Feedback Control on a UH-60 Black Hawk

Praneet Vayalali PhD Student
Michael McKay PhD Student
Jayanth Krishnamurthi PhD Graduate (Summer 2018)
Farhan Gandhi Redfern Chair in Aerospace Engineering
Center for Mobility with Vertical Lift (MOVE)
Rensselaer Polytechnic Institute
Troy, NY United States

ABSTRACT

The present study proposes an augmentation to the existing control mixing on the UH-60 Black Hawk to utilize the horizontal stabilator as an available control effector in the feedback loop to compensate for locked-in-place failure in the main rotor swashplate actuators. This modification has previously been shown to work in an adaptive sense, where once failure is detected the control mixing is remapped in flight. Now it is shown to perform well when the defined mixing includes the stabilator for all time, including the undamaged case, removing the need to detect and identify specific failures on the aircraft. Further investigation considered the benefit of allowing for more or less longitudinal authority to be given to the stabilator in different flight conditions, which include main rotor swashplate actuators locked-in-place, in the context of handling qualities ratings for the aircraft in pitch attitude and vertical rate response. Post-failure, the aircraft is demonstrated to retain level 1 performance in the pitch axis, whereas only aft actuator failure remains level 1 in the vertical rate response. Both cases show general improvement in handling qualities ratings with increased authority given to the horizontal stabilator. Finally, the aircraft is simulated flying a trajectory to a recoverable aircraft state, where the descent rate and forward speed are appropriate for a rolling landing.

NOTATION

$\vec{x}$	State Vector
$\vec{u}$	Control Stick Input Vector
δ_{lat}	Lateral Stick
δ_{lon}	Longitudinal Stick
δ_0	Collective Stick
δ_{ped}	Pedal Stick
$\delta_{throttle}$	Throttle
θ_0	Collective Pitch
θ_{1c}	Lateral Cyclic Pitch
θ_{1s}	Longitudinal Cyclic Pitch
θ_{ped}	Tail Rotor Collective Pitch
θ_{slew}	Stabilator Slew Schedule Pitch Incidence
s_{lat}	Lateral Actuator Position
s_{fwd}	Forward Actuator Position
s_{aft}	Aft Actuator Position
s_{ped}	Pedal Actuator Position
s_{fail}	Failed Actuator Position
$M_{\theta/S}$	Mechanical Mixer
$M_{S/u}$	Control Mixer
HQ	Handling Quality

Presented at the Vertical Flight Society 75th Annual Forum & Technology Display, Philadelphia, Pennsylvania, May 13–16, 2019.

INTRODUCTION

Aircraft survivability in the event of component failure or some loss of control effectiveness is an important area of research, particularly in control system design. For fixed wing aircraft, utilization of control redundancy has been explored for retaining aircraft stability despite a loss or degradation in control surface performance. This work is contained largely in the Air Force *Self-Repairing Flight Control System Program* (SRFCS), which resulted in the design and testing of a reconfigurable modified pseudo-inverse type control mixer which was able to maintain trimmed flight despite failure or loss of a control surface (Refs. 1–3), as well as the Reconfigurable Control for Tail-less Fighter Aircraft (RESTORE), which highlighted the abilites of a neural network to reconfigure aircraft control laws when a control effector was locked-in-place (Ref. 4).

Fixed wing aircraft are generally the focus of studies on control redundancy and aircraft survival. Though rotorcraft studies do exist in the literature, the number of articles is limited. Hess (Ref. 5) attributes this deficiency to the lack of redundant control effectors found on conventional rotorcraft, in the same work the author presents a pseudo-sliding mode control system for the UH-60A in hover, demonstrating robustness to variation in actuators, control system, vehicle characteristics, and sensors (also showing a degradation in the vehicle handling qualities). Other rotorcraft focused studies include Heiges (Ref. 6), where proven fixed-wing reconfiguration strategies were shown to be effective if sufficient redundancy exists in the system, as well as Enns and Si (Ref. 7),

which focused on a reconfigurable swashplate control for fault tolerance.

Recently, Reddinger and Gandhi (Ref. 8) explored control reconfiguration on compound helicopters to compensate for swashplate actuator failure in trim. Vayalali et al (Ref. 9) continued this work, examining the effectiveness of the horizontal stabilator on a UH-60 Black Hawk to compensate for certain swashplate actuator *locked-in-place* failures. The study concludes that introducing the stabiltor as a control input in the feedback loop for the control system *post-failure* allows the system to recover in flight simulation.

Previously, the controller designed was adapted once failure occurred to introduce the stabilator into the feedback loop at the time of actuator locking. The present study examines a control design where the horizontal tail is always present in the feedback control loop, even on the undamaged aircraft. With this control architecture, the trade-offs of including redundant controls in the feedback control laws for the aircraft at all times are studied in terms of the handling qualities ratings for the aircraft.

APPROACH

Modeling

A UH-60A Black Hawk simulation model developed by Krishnamurthi and Gandhi (Ref. 10), which is a derivative of Sikorsky's GenHel model (Ref. 11), is used in this study. The model includes a non-linear, blade element representation of a single main rotor with articulated blades using airfoil table lookup. The blades themselves are approximated to be rigid, undergoing rotations about offset hinges. The 3-state Pitt-Peters dynamic inflow model (Ref. 12) is used to represent the induced velocity distribution on the rotor disk, while the tail rotor thrust and torque are based on the closed-form Bailey rotor (Ref. 13) with a Pitt-Peters 1-state dynamic inflow model. The rigid fuselage and empennage (horizontal and vertical tail) forces and moments are implemented as look-up tables based on wind tunnel data from the GenHel model (Ref. 11). A simple 3-state turbine engine model given by Padfield (Ref. 14) is used for the propulsion dynamics, with the governing time constants approximated based on the GenHel engine model. The governing equations of motion are given by

$$\begin{aligned} \dot{\vec{x}} &= f(\vec{x},\vec{u}) \\ \vec{y} &= g(\vec{x},\vec{u}) \end{aligned} \tag{1}$$

where $\vec{y}$ is a generic output vector. The state vector $\vec{x}$, is given by

$$\begin{aligned} \vec{x} = [&u,v,w,p,q,r,\phi,\theta,\psi,X,Y,Z,\beta_0,\beta_{1s},\beta_{1c},\beta_d,\dot{\beta}_0,\dot{\beta}_{1s},\dot{\beta}_{1c}, \\ &\dot{\beta}_d,\lambda_0,\lambda_{1s},\lambda_{1c},\lambda_{0_{TR}},\Omega,\chi_f,Q_e]^T \end{aligned} \tag{2}$$

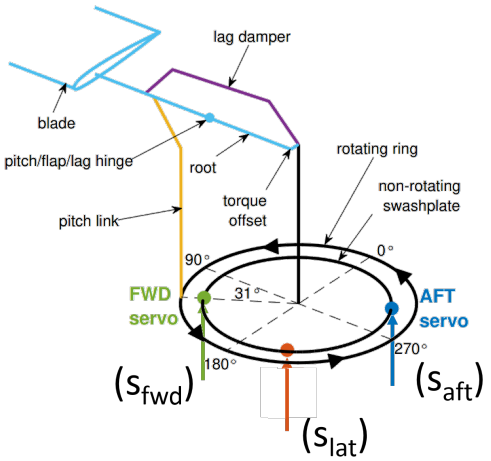

Fig. 1. Swashplate Servo Actuator Geometry

The state vector comprises of :

- 12 fuselage states $(u,v,w,p,q,r,\phi,\theta,\psi,x,y,z)$,
- 11 rotor states $(\beta_0,\beta_{1s},\beta_{1c},\beta_d,\dot{\beta}_0,\dot{\beta}_{1s},\dot{\beta}_{1c},\dot{\beta}_d,\lambda_0,\lambda_{1s},\lambda_{1c})$,
- 1 tail rotor inflow state $(\lambda_{0_{TR}})$, and
- 3 engine states (Ω,χ_f,Q_e).

The control stick input vector is given by

$$\vec{u} = [\delta_{lat},\delta_{lon},\delta_{col},\delta_{ped},\delta_{throttle}]^T \tag{3}$$

Validation of the baseline simulation model was performed in Ref. 10 against a trim sweep of flight test and GenHel data from Ref. 15, for a gross weight of 16,000 lbs and altitude of 5,250 ft.

Actuator geometry

Collective, lateral and longitudinal blade pitch $(\theta_0,\theta_{1c},\theta_{1s})$ are achieved by moving the base of the pitch link from the reference plane of the level swashplate. The non-rotating swashplate orientation is fully defined by the height of the swashplate servo actuators, where s_{lat}, s_{fwd}, and s_{aft} actuate to transmit pilot control, as shown in Fig. 1. The servo actuator positions are related to the blade pitch controls $(\theta_0,\theta_{1c},\theta_{1s})$ by Eqs. 4-9. These equations demonstrate that the independent control of θ_0, θ_{1c}, and θ_{1s} is attainable with full control of s_{lat}, s_{fwd}, and s_{aft}.

$$\theta_{1c} \propto \frac{(s_{fwd}+s_{aft})}{2} - s_{lat} \tag{4}$$

$$\theta_{1s} \propto \frac{(s_{fwd}-s_{aft})}{2} \tag{5}$$

$$\theta_0 \propto \frac{(s_{fwd}+s_{aft})}{2} \tag{6}$$

$$s_{lat} \propto \theta_0 - \theta_{1c} \tag{7}$$

$$s_{fwd} \propto \theta_0 + \theta_{1s} \tag{8}$$

$$s_{aft} \propto \theta_0 - \theta_{1s} \tag{9}$$

To produce an increase in collective pitch (θ_0) without changing the cyclic pitches, all three actuators need to be raised the same amount. Isolated increases in longitudinal cyclic pitch (θ_{1s}) result from a differential between the forward and aft actuators, while isolated lateral cyclic pitch (θ_{1c}) variation is accomplished by changing the lateral actuator position.

The servo naming convention is given relative to the primary effect that each actuator has on the flapping of the rotor (Fig. 1). Increases in the forward actuator height will increase longitudinal cyclic pitch and the rotor will flap up in the front of the disk, increases in the lateral actuator height will increase lateral cyclic pitch and lateral blade flapping, and increases in the aft actuator height will reduce longitudinal cyclic pitch and produce a higher flapping angle in the rear of the disk.

Servo actuator failure

The type of actuator failure addressed in the present study is referred to as a *locked condition*, where the input signal to a control actuator yields no response, as the actuator position is locked in place. This type of actuator failure results in a loss of independent control of the three blade pitches ($\theta_0, \theta_{1c}, \theta_{1s}$) as seen in Eqs. 4-9. Independent control of one is possible (over a certain range), but the two remaining blade pitches are governed by a constraint equation. For example, in the case of s_{fwd} or s_{aft} locked in place, lateral cyclic pitch (θ_{1c}) remains independently controllable (by use of s_{lat}), while longitudinal cyclic (θ_{1s}) and collective pitch (θ_0) become coupled. However, this issue can be mitigated by including redundant control effectors in the feedback loop throughout operation. In the present study, the horizontal stabilator is allocated along with swashplate longitudinal cyclic pitch (θ_{1s}), which is mapped from the longitudinal stick input from the pilot (δ_{long}).

Control system design

The control system for the simulation model is designed based on model-following linear dynamic inversion (DI) (Ref. 16). Model-following concepts are widely used in modern rotorcraft control systems for their ability to independently set feed-forward and feedback characteristics. The DI controller schedules the model with flight condition to eliminate the need for feedback gain scheduling due to similar error dynamics over different flight regimes. The controller is therefore applicable to a wide range of flight conditions (Refs. 16, 17). In the inner loop, the response type to pilot input is designed for Attitude Command Attitude Hold in the roll and pitch axis, where pilot input commands a change in roll and pitch attitudes ($\Delta\phi_{cmd}$ and $\Delta\theta_{cmd}$) and returns to the trim values when input is zero. The heave axis response type is designed for Rate Command Altitude Hold, where pilot input commands a change in rate-of-climb and holds current altitude when the rate-of-climb is zero. The yaw axis response type is designed for Rate Command Direction Hold, where pilot input commands a change in yaw rate and holds current heading when the yaw rate command is zero. The response type for the outer loop is Translational Rate Command, Position Hold, where pilot inputs command a change in ground speed and hold current inertial position when inputs are zero. With the implementation of the outer loop, the pilot input does not directly command $\Delta\phi_{cmd}$ *and* $\Delta\theta_{cmd}$ as in the inner loop CLAW. Rather, they are indirectly commanded through the desired ground speeds. For designing the CLAWS, the full 27-state linear model is reduced to an 8-state quasi-steady model whose state and control vectors are given by

$$\begin{aligned} \vec{x}_r &= [u, v, w, p, q, r, \phi, \theta]^T \\ \vec{u}_r &= [\delta_{lat}, \delta_{lon}, \delta_{col}, \delta_{ped}]^T \end{aligned} \tag{10}$$

Currently the main rotor RPM (Ω) is regulated via the throttle input determined by the RPM Governor. Therefore, $\delta_{throttle}$ is truncated from the original control input vector. A more detailed explanation of the control system design is available in (Ref. 10).

Control Mixer

In the baseline simulation model, the control input vector $\vec{u}$ is comprised of two parts, namely $\vec{u}_{trim}$ and $\Delta\vec{u}$, where $\vec{u}_{trim}$ represents the reference trim input (determined by an off-line trim routine) to the aircraft and $\Delta\vec{u}$ denotes the change in control inputs from the feedback control laws. The trim control inputs ($\vec{u}_{trim}$) are mapped to the main rotor swashplate servo actuators ($s_{lat}, s_{fwd}, s_{aft}$), and the tail rotor servo actuator (s_{ped}) through a control mixer, $\tilde{M}_{S/u}$ as shown in Eq. 11.

$$\vec{S}_{trim} = \tilde{M}_{S/u}\vec{u}_{trim} \quad \text{where} \quad \vec{S}_{trim} = [s_{lat}, s_{fwd}, s_{aft}, s_{ped}]^T_{trim} \tag{11}$$

Similarly, $\Delta\vec{u}$ is mapped to the actuators through a control mixer ($\hat{M}_{S/u}$) as in Eq. 12.

$$\Delta\vec{S} = \hat{M}_{S/u}\Delta\vec{u} \quad \text{where} \quad \Delta\vec{S} = [\Delta s_{lat}, \Delta s_{fwd}, \Delta s_{aft}, \Delta s_{ped}]^T \tag{12}$$

The summation of the trim servo actuator inputs ($\vec{S}_{trim}$) and the change in servo actuator inputs ($\Delta\vec{S}$) from $\Delta\vec{u}$ are in turn mapped to the collective, lateral and longitudinal blade pitch ($\theta_0, \theta_{1c}, \theta_{1s}$), and tail rotor collective pitch (θ_{tr}), through mechanical mixing ($M_{\theta/S}$) with an additional bias vector ($\vec{\theta}_{bias}$) as shown in Eq.13 (Ref. 11).

$$\vec{\theta} = M_{\theta/S}(\vec{S}_{trim} + \Delta\vec{S}) + \vec{\theta}_{bias} \tag{13}$$

In previous work published by the authors (Ref. 9), the control mixer was adapted based on the fault that had occured in the swashplate. In the present study, no adaptation occurs in the control mixing. That is, the horizontal stabilator is always used as a control surface in concert with the longitudinal cyclic input to the rotor for commanded longitudinal acceleration. Equation 12 now takes the form as shown in Eq.14:

$$\Delta\vec{S} = \hat{M}_{S/u}\Delta\vec{u} \quad \text{where} \quad \Delta\vec{S} = [\Delta s_{lat}, \Delta s_{fwd}, \Delta s_{aft}, \Delta s_{ped}, \Delta s_{stab}]^T \tag{14}$$

and the control mixer $\hat{M}_{S/u}$ is given by Eq. 15:

$$\hat{M}_{S/u} = \begin{bmatrix} m_{11} & 0 & m_{13} & 0 \\ 0 & m_{22} & m_{23} & m_{24} \\ 0 & m_{32} & m_{33} & m_{34} \\ 0 & 0 & m_{43} & m_{44} \\ 0 & m_{52} & 0 & 0 \end{bmatrix} \tag{15}$$

Here, the entry m_{52} represents the mapping from δ_{long} to the stabilator actuator. In the mechanical mixing ($M_{\theta/S}$), this displacement of the stabilator actuator is mapped directly to the change in incidence of the horizontal tail. It should be noted that this commanded change in stabilator incidence is added to the nominal incidence per the UH-60A slew schedule according to the current airspeed of the vehicle. A more detailed presentation of this architecture is provided in Ref. 9.

RESULTS AND DISCUSSION

Robust Control Effectiveness

The authors have previously demonstrated that when a swashplate actuator locks in place, reconfiguration of the control laws to include the stabilator as an active effector in the feedback loop allows the aircraft to recover from the transient effects. It is worth noting that the stabilator slew rate is limited to 8°/sec. With the present framework, the stabilator is always being utilized, the performance of the closed loop system in this configuration can be examined both pre- and post-failure.

First, the ability of the pristine aircraft to track a commanded change in flight speed from 80 to 120 kts is presented in Fig. 2.

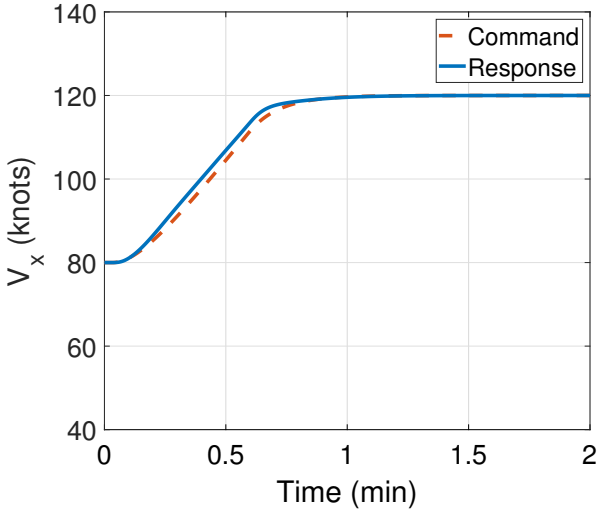

Fig. 2. Time History of Forward Flight Speed

Clearly, the aircraft is able to track the reference signal quite well. Note that this simulation result is not remarkably different from the baseline control laws that don't make use of the stabilator in feedback. The key difference between this simulation and the baseline case is the utilization of the horizontal tail, which is portrayed in Fig. 3.

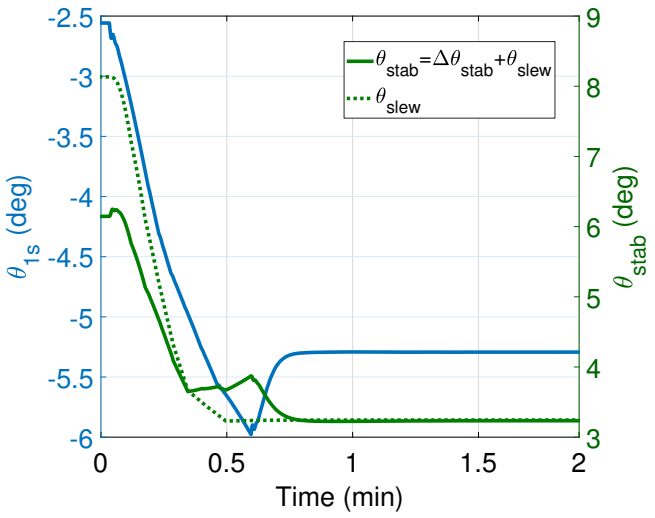

Fig. 3. Time History of Longitudinal Cyclic, θ_{1s} and Stabilator, θ_{stab}

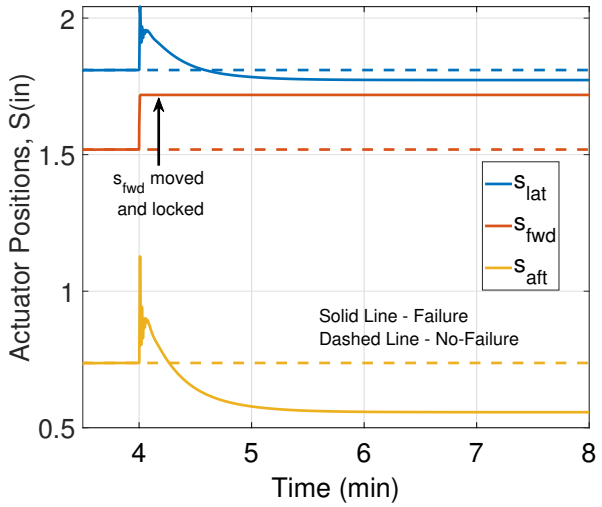

Fig. 4. Time History of Swashplate Actuator Positions

Here, observe that this 40 kt increase in flight speed involves a change not only in the longitudinal cyclic, but also the stabilator incidence. Important to note is that the dotted green line represents the flight speed scheduled incidence of the stabilator, but with the mixing now defined as in Eq. 15, the stabilator incidence reflects the tracking error in the flight speed.

After the performance of the new control laws on the pristine aircraft are deemed adequate, an examination of the closed loop performance in the event of a swashplate actuator failure can be undertaken. Figure 4 shows the time history of the swashplate actuators, where the forward actuator experiences a locked failure at $t = 4$ minutes, while cruising at 120 kts.

In the time histories, observe that the forward actuator, s_{fwd} is simulated to move out of trim by 0.2 inches before being

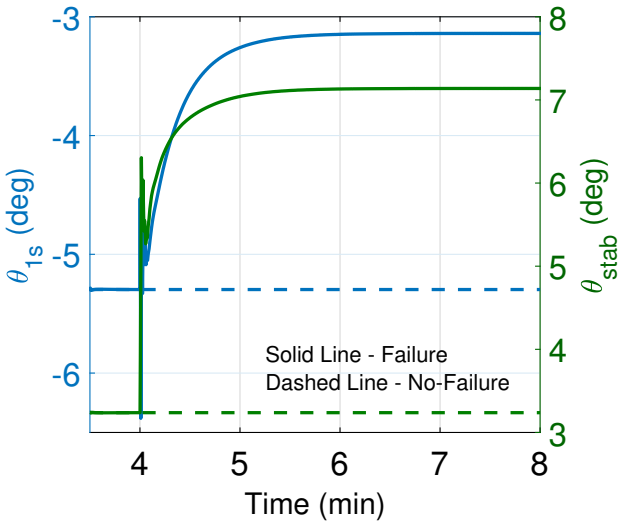

Fig. 5. Time History of Longitudinal Cyclic, θ_{1s} and Stabilator, θ_{stab}

locked in place in order to perturb the aircraft from its steady state. The aft and lateral actuators are then seen moving in order to recover the aircraft state, eventually settling to a new steady state for the aircraft, which is still maintaining 120 kts cruise speed. The aft actuator position, s_{aft} decreases in order to hold the collective pitch, θ_0.

As the forward actuator, s_{fwd} is raised by 0.2 inches and locked out of trim, the longitudinal cyclic pitch, θ_{1s} becomes less negative causing the rotor to flap back, which results in the main rotor producing a nose-up pitching moment. In order to compensate, the stabilator is moved to generate a nose-down pitching moment. Figure 5 shows the contributions of the controls in the longitudinal axis, which demonstrate the utilization of both longitudinal cyclic pitch and stabilator incidence to return the aircraft to steady state.

Pitch Authority Sharing

The previous results establish the effectiveness of the control architecture for one example of the control mixer, or one case of relative longitudinal authority sharing between the swashplate and stabilator. However, based on the framework in Eq. 15, the authority in the longitudinal axis can be changed by varying the weights on the terms relating the longitudinal stick input to the various actuators. Notionally, this can take the form of Eq. 16.

$$\hat{M}_{S/u} = \begin{bmatrix} m_{11} & 0 & m_{13} & 0 \\ 0 & \beta m_{22} & m_{23} & m_{24} \\ 0 & \beta m_{32} & m_{33} & m_{34} \\ 0 & 0 & m_{43} & m_{44} \\ 0 & \gamma m_{52} & 0 & 0 \end{bmatrix} \tag{16}$$

The values of β and γ in this matrix define (in conjunction with the pre-existing m_{x2} terms) the deflection of the swashplate actuators and stabilator, respectively. The splitting of authority in the longitudinal axis by the controller is captured by the relative values of β and γ. The simulation results presented in the previous section represent the case where β and γ take on their nominal value of 1, which is identical to the controller presented in Ref. 9 after adaptation has occurred post-failure.

The effects of authority sharing can be examined by variation in the values of β and γ. This can generally be accomplished by the relation $\gamma = 1 - \beta$ and exploring all values of $\beta \in [0,1]$. However, given the restriction of the stick input (δ) to a range of $0-100\%$, the present study considers instead a bilinear relationship between β and γ, defined as (with use of parameter α, which can take values between 0 and 1, inclusive)

$$\beta = \begin{cases} 1 & 0 \le \alpha \le 0.5 \\ 2(1-\alpha) & 0.5 < \alpha \le 1 \end{cases}$$
$$\gamma = \begin{cases} 2\alpha & 0 \le \alpha \le 0.5 \\ 1 & 0.5 < \alpha \le 1 \end{cases} \tag{17}$$

This variation allows for different relative sharing values to be accounted for even in the presence of limitations in the stick deflection. Note that lower values of α dictate less authority being given to the stabilator, with $\alpha = 0$ denoting the nominal control mixing for the UH-60 Black Hawk. As α increases, more authority is given to the stabilator while the swashplate retains its nominal authority, up until $\alpha = 0.5$, where the control mixing is defined as it was for the adapted case in Ref. 9. For values of α ranging from 0.5-1, the stabilator retains a nominal authority, while the swashplate authority is decreased to the limit case of $\alpha = 1$, where only the stabilator is used in the longitudinal control channel. Parameterizing each coefficient by a single variable α allows for a single degree of freedom for variation in the control mixer, which simplifies the analysis presented herein.

With the control mixer ($M_{S/u}$) defined with the choice of α, the mechanical mixer ($M_{\theta/S}$) defined by the geometry of the aircraft, and the control laws defined by the model-following linear dynamic inversion controller, a closed-loop model of the aircraft system can be generated for different operating conditions (failure cases, flight speeds, etc.). From these models, target tracking and acquisition handling qualities ratings can be generated for the pitch axis (Fig. 6).

Figure 6 shows the pitch attitude bandwidth and phase delays for different forward speeds, V_x, and variation of longitudinal authority between the stabilator and swashplate, α. The solid markers represent the baseline aircraft while the hollow thin and thick markers show for the failed forward and aft actuator cases respectively.

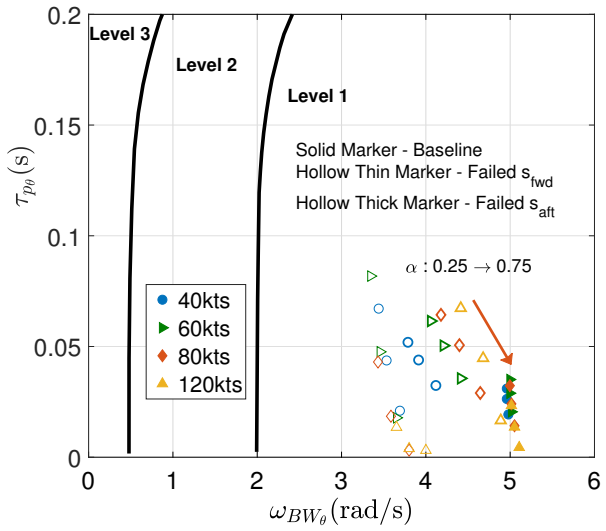

Fig. 6. Pitch Attitude Bandwidth and Phase Delay Based on ADS-33E HQ Requirements for Combat/Target Tracking in Forward Flight

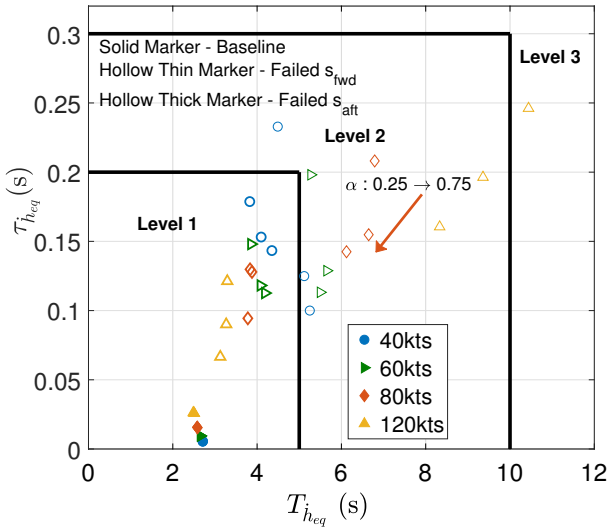

Fig. 7. Vertical Rate Response ADS-33E HQ Requirements in Forward Flight

Overall, the handling qualities ratings fall in level 1 for all cases considered, both pre- and post-actuator failure. Intuitively, the aircraft performance degrades once an actuator locks in place, this is reflected by the leftward movement of the hollow markers relative to the solid markers along the bandwidth axis.

One distinction that can be made between the pristine (solid marker) and failure (hollow marker) cases is the increase in handling qualities variation with the sharing parameter α. When failure occurs, the ratings given in Fig. 6 show a clear trend toward more desirable aircraft performance with increasing α, or more longitudinal authority being given to the stabilator. This variation is attributed to the relative improvement in speed of response when the stabilator is used as the primary effector in the longitudinal axis (larger values of α). Because the stabilator is able to act quickly (with no reliance on rotor flap dynamics) and directly (minimal off-axis effects), the closed loop system in general sees an improvement in the overall aircraft rating with increased stabilator authority.

Clearly, the present control system design is able to retain level 1 handling qualities ratings for the pitch axis even in the event of a locked swashplate actuator. However, the other dynamic axes for the aircraft are also impacted as a result of the new couplings arising from the locked position of the actuator, particularly the coupling between collective and longitudinal cyclic pitch in the case of forward or aft actuator failure (see Eqs. 5-6). For this reason, the system handling qualities in the heave axis must be considered as well (Fig. 7).

This figure shows the phase delays, $\tau_{\dot{h}_{eq}}$ and time constants, $T_{\dot{h}_{eq}}$ for different forward speeds, V_x, and variation of longitudinal authority between the stabilator and swashplate, α. The solid markers represent the baseline aircraft while the hollow thin and thick markers show for the failed forward and aft actuator cases respectively.

Again, observe that the baseline aircraft (solid marker) has very desirable performance for all of the flight speeds and sharing cases considered in the present study. There is no significant change in the ratings for the aircraft with change in α because the pristine aircraft sees no real change when the stabilator is used in the longitudinal axis. The observed variation with flight speed has to do with the change in aircraft control sensitivity from δ_{col} to heave acceleration with flight speed, which is displayed in Fig. 8.

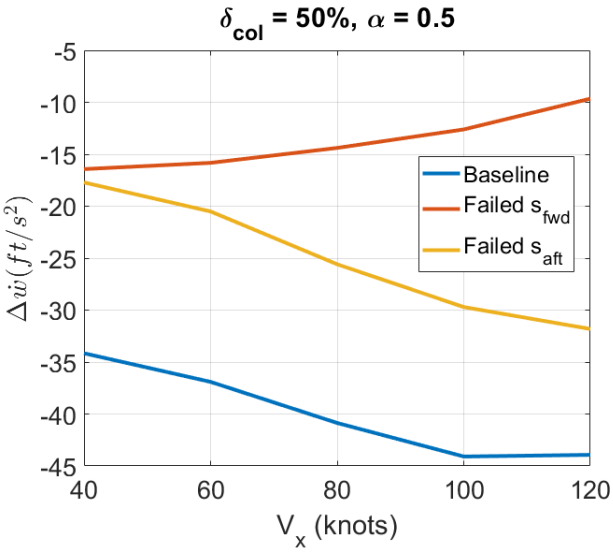

Fig. 8. Change in Body Z Acceleration, $\Delta\dot{w}$ with Forward Speed, V_x

As was the case in the pitch axis handling qualities, once an actuator fails, there is a degradation in the system performance. In the heave axis, this degradation tends to be more

severe, to the point that cases of forward actuator failure (hollow thin markers) depart the level 1 region of Fig. 7. Again, there is a notable improvement in the handling qualities of the damaged aircraft with increasing α, which is attributed to the increased use of the stabilator versus the swashplate, which reduces the impact of the aforementioned control couplings present post-failure.

Another observation in Fig. 7 is the variation in the handling qualities with flight speed, notably the different trends for different failure cases. For forward actuator failure (thin hollow markers), an increase in flight speed for a given value of α results in an increase in the time constant for the heave response, and an overall degradation in the handling qualities themselves. Conversely, in the case of aft actuator failure (thick hollow markers), the time constant generally decreases with increasing flight speed, corresponding to an improvement in the handling qualities rating for the aircraft in heave. This difference between the two failure cases can be explained by the sensitivity of the aircraft heave acceleration to δ_{col} with flight speed, shown in Fig. 8 (for $\alpha = 0.5$ and $\delta_{col} = 50\%$ for the linearized system).

Clearly, when either the forward or aft actuator locks in place, the ability of the aircraft to generate a heave acceleration with collective input decreases substantially ($48.2 - 51.9\%$) relative to the pristine case at 40 kts. More importantly, the aircraft sensitivity to collective stick exhibits different trends with forward flight speed depending on which actuator has failed. These trends correspond directly to the difference in behavior seen in Fig. 7, where forward actuator failure cases perform more poorly with increasing flight speed and aft actuator failure cases improve. This dichotomy can be explained by the control coupling that arises from each case of actuator failure, which is captured in Fig. 9.

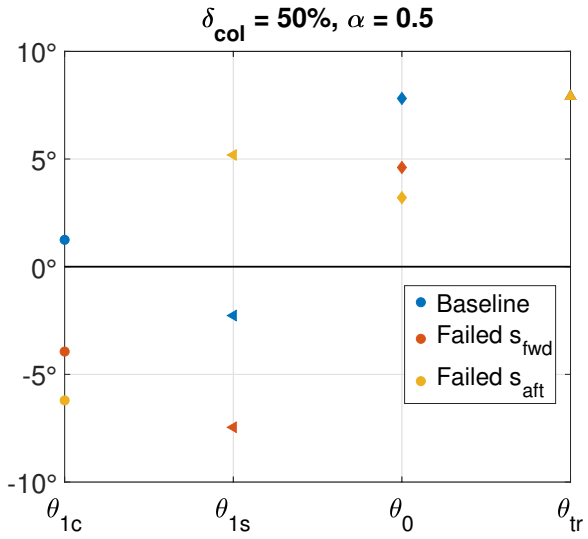

Fig. 9. Blade Pitch Positions for 50% Collective Stick and Full Authority to Swashplate and Stabilator, α = 0.5

Figure 9 shows the result of the control mixing between the stick input δ_{col} and the rotor pitches (θ_0, θ_{1s}, θ_{1c}) and tail rotor pitch (θ_{tr}) for the pristine and actuator failure cases. Specifically, the figure shows the result of a 50% collective stick input with $\alpha = 0.5$. Note that these results are flight speed invariant and depend only on the mixing matrices presented earlier. When a step input in vertical velocity is put into the system, the heave control channel compensates with a change in the collective stick input δ_{col}. This collective input results in the changes in blade and tail rotor pitch shown with the blue markers (pristine case) in Fig. 9 (albeit scaled from different stick input magnitude). However, once failure occurs in the swashplate, the resultant blade pitches for the same collective input changes, resulting in the red and yellow markers for forward and aft actuator failure cases, respectively.

In order to explain the differences between forward and aft actuator failure cases in the context of Fig. 7, the resultant longitudinal cyclic pitch from the same collective input can be examined. In a notional forward flight case, the UH-60 trims with a positive longitudinal flap (β_{1c}), which tilts the rotor thrust forward to propel the aircraft and overcome drag. With a failed actuator, a deflection in the collective stick input results in a change in the longitudinal cyclic pitch (θ_{1s}), which in turn will result in a change in the longitudinal flap of the rotor. However, from Fig. 9, observe that δ_{col} results in different signed changes in θ_{1s} and consequently β_{1c}, which will tilt the rotor plane either forward (Fig. 10) or backward (Fig. 11) relative to the baseline operating condition. This tilting redirects the thrust either toward or away from the vertical direction, depending on which actuator has failed.

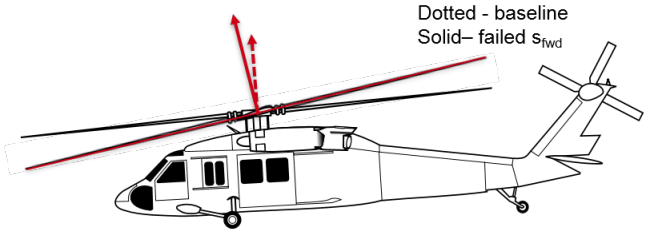

Fig. 10. Effect of Collective Stick under Failed Forward Actuator

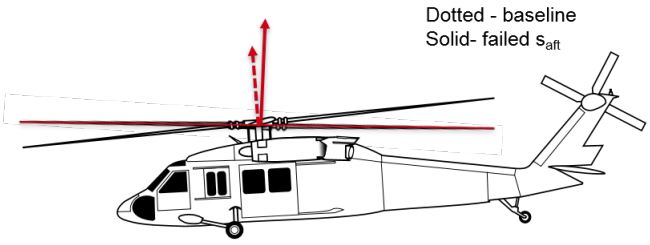

Fig. 11. Effect of Collective Stick under Failed Aft Actuator

Consider the case of aft actuator failure. When the actuator is

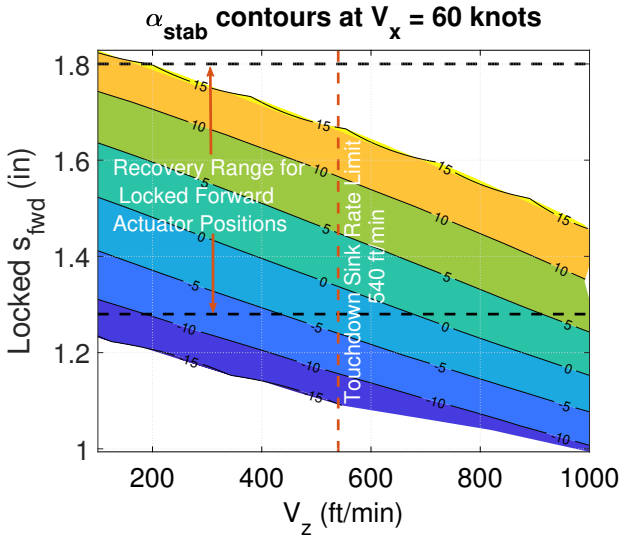

Fig. 12. Velocity Trim Sweep Showing Forward Actuator Positions, s_{fwd} for Varying Sink Rates at a Forward Speed, V_x = 60 knots

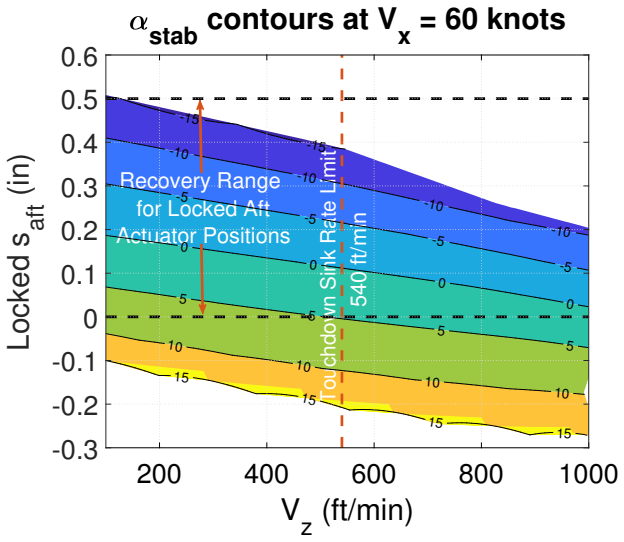

Fig. 13. Velocity Trim Sweep Showing Aft Actuator Positions, s_{aft} for Varying Sink Rates at a Forward Speed, V_x = 60 knots

locked and an increase in δ_{col} is commanded, it results in an increase in θ_{1s}, which causes the rotor to flap back. Provided that the rotor is flapped forward to maintain propulsive thrust, this flap back of the rotor plane results in the thrust (which is augmented by the increase of θ_0) being tilted more toward vertical, which improves the vertical acceleration of the aircraft (Fig. 11). The opposite tilting of the rotor plane occurs with failure of the forward actuator (Fig. 10), consequently the height response of the aircraft is degraded relative to the aft actuator failure. The sensitivity of this height response to the longitudinal flap of the rotor accounts for the variation with flight speed seen in Fig. 8.

Recovery

Another important consideration for fault tolerant systems is the ability to recover the aircraft once damage has occurred. In particular, the ability to descend with a locked actuator given the coupling that arises between the collective and longitudinal cyclic pitch of the rotor is important to consider. Previously (Ref. 9), the authors have considered the ability of the aircraft to slow to an allowable rolling landing speed per the UH-60 operations manual (Ref. 18). In the present study, the ability of the aircraft to achieve an acceptable sink rate (540 ft/min on flat ground for gross weight $\leq$ 16,825 lb) for landing is examined.

The authors have previously shown that using the stabilator post-actuator failure allows for the aircraft to be slowed to below 60 kts cruise speeds, the maximum allowable rolling landing speed for the aircraft. Figures 12 and 13 show the steady state attainable sink rates for the aircraft at 60 kts cruise with locked forward and aft actuator positions, respectively with contours of stabilator angle of attack (α_{stab}).

Both figures show that within the recoverable range of locked forward and aft actuator positions reported in Ref. 9, there exists a stabilator position for which it is possible to achieve an acceptable sink rate. This suggests that the aircraft should be able to slow and descend to an appropriate flight state at which it can land, thus recovering the airframe safely.

Figures 14-17 show the simulation results of the aircraft after failure of the forward actuator, once the aircraft has been slowed to 40 kts (with $\alpha = 0.5$). At $t = 4$ minutes, the aircraft is commanded to begin descending at 350 ft/min (Fig. 14).

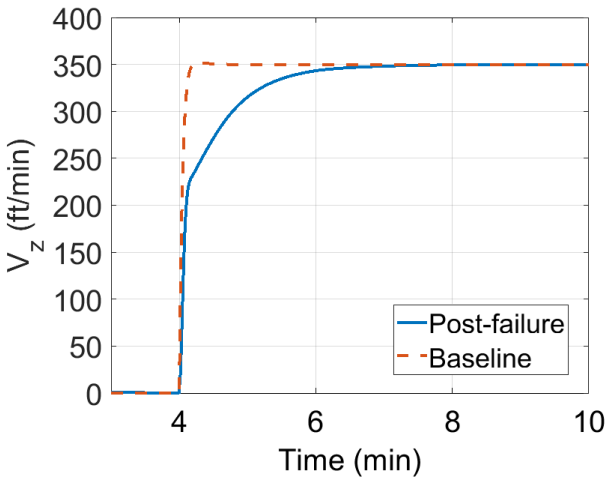

Fig. 14. Time History of Sink Rate

The damaged aircraft is unable to track the command signal as well as the baseline case (dashed vs solid line in Fig. 14), primarily due to the control coupling between collective and longitudinal cyclic pitch discussed previously. Figures 15 and 16 show the time history of these control inputs, respectively, which explains the slower behavior of the curve in Fig. 14 relative to the baseline aircraft.

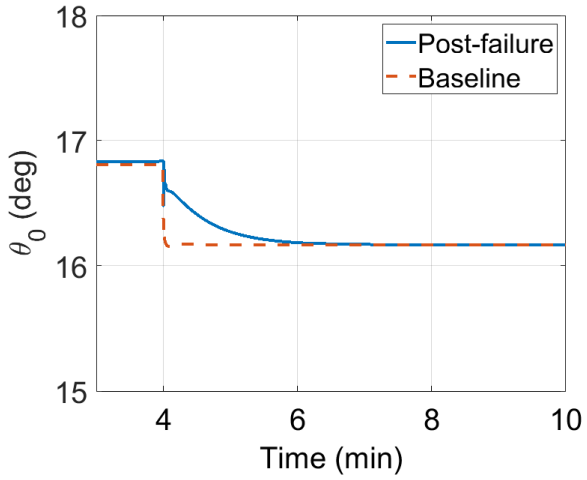

Fig. 15. Time History of Collective Pitch, θ_0

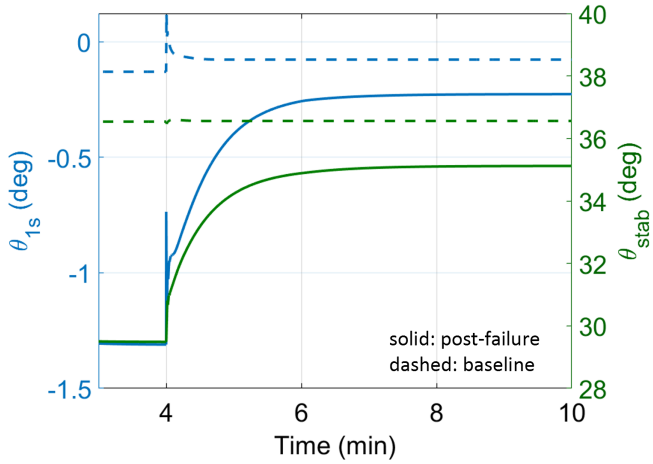

Fig. 16. Time History of Longitudinal Cyclic, θ_{1s} and Stabilator, θ_{stab}

Observe in Fig. 15 that the controller commands an immediate decrease in the collective pitch input, a signal which the pristine aircraft (dashed line) tracks well. Instantaneously, because the only appreciable tracking error in the closed loop system is the vertical velocity, the damaged aircraft tracks this decrease in collective pitch, which is accomplished by a lowering of the δ_{col} input. However, because the forward actuator in the swashplate has been locked in place, a change in the collective stick input corresponds to not only a change in the collective pitch of the rotor, but also a change in the longitudinal cyclic pitch (Fig. 16). This change in θ_{1s} results in a flap back of the main rotor, which tends to slow the aircraft down (Fig. 17). Once this error becomes substantially large, the controller compensates with an increase in δ_{long}, which changes the collective pitch setting as well as θ_{1s}. This coupling slows the aircraft response in Fig. 14 substantially relative to the baseline case, where the couplings are inconsequential.

Overall, the simulation demonstrates the capability of the aircraft to achieve a steady state sink rate (Fig. 14) while maintaining forward flight speed (Fig. 17), which ensures the usability of the horizontal tail. Note that in Fig. 16, the stabilator incidence changes in order to augment the longitudinal response for the aircraft, which alleviates the control coupling and allows for the aircraft to achieve the commanded sink rate. From previous discussion, increasing the authority given to the stabilator (increasing α) should improve this system response further. Nonetheless, Figs. 14-17 illustrate the closed loop system ability to stabilize to a state in which the airframe could be recovered.

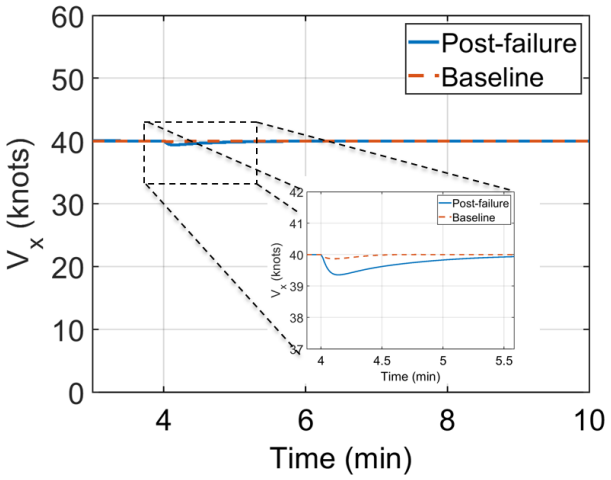

Fig. 17. Time History of Forward Speed

CONCLUSIONS

The present study proposes an augmentation to the existing control mixing on the UH-60 Black Hawk in order to utilize the horizontal stabilator as an available control effector in the feedback loop to compensate for locked-in-place failure in the swashplate actuators. This modification has previously been shown to work in an adaptive sense, where once failure is detected the mixing is adjusted in flight. Now it is shown to perform well when the defined mixing includes the stabilator for all time, including the undamaged case, which would obviate the need for a fault detection and identification system for the aircraft.

Further investigation considered the benefit of allowing for more or less longitudinal authority to be given to the stabilator in different flight conditions in the context of handling qualities ratings for the aircraft in pitch attitude and vertical rate response. In the pitch response, even post-failure, the handling qualities ratings remained level one for all levels of authority sharing between stabilator and swashplate at the cruise speeds considered. In the vertical rate response, the aircraft remained level 1 for all levels of authority sharing only for the pristine aircraft and aft actuator failure, falling to level 2 in all cases for forward actuator failure (again at the considered flight speeds). It is also noted that the handling qualities ratings show notable variation with flight speed, showing general improvement in the pitch axis with flight speed for the pristine and failed aircraft (both cases), whereas in the vertical

rate response increasing flight speed improved handling qualities ratings for the failed aft actuator and degraded ratings for the forward actuator case. Generally, biasing the mapping of longitudinal stick input more to the stabilator resulted in more desirable handling qualities ratings in both the pitch and heave axes for the failed aircraft, with no significant change in the ratings for the pristine case. This indicates that where feasible (in moderate to high speed cruise), the stabilator should be used in the longitudinal axis. However, full use of the stabilator (no use of longitudinal cyclic) is not desirable as it removes the control redundancy entirely and makes the aircraft vulnerable to failure in the stabilator.

Finally, steady-state trim solutions exist for a range of locked actuator positions at varying sink rates and stabilator angle of attacks for the maximum acceptable forward speed for rolling landing of 60 kts. The aircraft is also simulated flying a trajectory to a recoverable aircraft state, where the descent rate (350 ft/min) and forward speed (40 kts) are appropriate for a rolling landing.

AUTHOR CONTACT

Praneet Vayalali	vayalp@rpi.edu
Michael McKay	mckaym2@rpi.edu
Jayanth Krishnamurthi	jayanth.krishnamurthi@lmco.com
Farhan Gandhi	fgandhi@rpi.edu

ACKNOWLEDGMENTS

This work is carried out at the Rensselaer Polytechnic Institute under the Army/Navy/NASA Vertical Lift Research Center of Excellence (VLRCOE) Program, grant number W911W61120012, with Dr. Mahendra Bhagwat and Dr. William Lewis as Technical Monitors. The authors would also like to acknowledge the Department of Defense and STI for sponsoring Mr. McKay through the National Defense Science and Engineering Graduate Fellowship.

REFERENCES

[1]R. A. Eslinger and P. R. Chandler, "Self-Repairing Flight Control System program Overview," in *Proceedings of the IEEE 1988 National Aerospace and Electronics Conference*, pp. 504–511 vol.2, May 1988.

[2]J. F. Stewart and T. L. Shuck, "Flight-Testing of the Self-Repairing Flight Control System Using the F-15 Highly Integrated Digital Electronic Control Flight Research Facility," tech. rep., NASA-TM-101725, 06 1990.

[3]M. Bodson and J. E. Groszkiewicz, "Multivariable Adaptive Algorithms for Reconfigurable Flight Control," *IEEE Transactions on Control Systems Technology*, vol. 5, pp. 217–229, March 1997.

[4]J. S. Brinker and K. A. Wise, "Flight Testing of Reconfigurable Control Law on the X-36 Tailless Aircraft," *Journal of Guidance, Control, and Dynamics*, vol. 24, no. 5, pp. 903–909, 2001.

[5]R. Hess, "A Framework for Robust Rotorcraft Flight Control Design," *Journal of the American Helicopter Society*, vol. 56, pp. 22004–1, 04 2011.

[6]M. W. Heiges, "Reconfigurable Controls for RotorcraftA Feasibility Study," *Journal of the American Helicopter Society*, vol. 42, no. 3, pp. 254–263, 1997.

[7]R. Enns and J. Si, "Helicopter Flight-Control Reconfiguration for Main Rotor Actuator Failures," *Journal of guidance, control, and dynamics*, vol. 26, no. 4, pp. 572–584, 2003.

[8]J. P. Reddinger and F. Gandhi, "Using Redundant Effectors to Trim a Compound Helicopter with Damaged Main Rotor Controls," in *American Helicopter Society 73rd Annual Forum Proceedings*, (Fortworth, TX), May 2017.

[9]P. Vayalali, M. Mckay, J. Krishnamurthi, and F. Gandhi, "Swashplate Actuator Failure Compensation for UH-60 Black Hawk in Cruise using Horizontal Stabilator," in *American Helicopter Society 74rd Annual Forum Proceedings*, (Phoenix, AZ), May 2018.

[10]J. Krishnamurthi and F. Gandhi, "Flight simulation and control of a helicopter undergoing rotor span morphing," *Journal of the American Helicopter Society*, vol. 63, no. 1, pp. 1–20, 2018.

[11]J. J. Howlett, "UH-60A Black Hawk Engineering Simulation Program. Volume 1: Mathematical Model," *NASA CR-166309*, 1981.

[12]D. A. Peters and N. HaQuang, "Dynamic Inflow for Practical Applications," *Journal of the American Helicopter Society*, vol. 33, pp. 64–66, Oct. 1988.

[13]F. Bailey Jr, "A Simplified Theoretical Method of Determining the Characteristics of a Lifting Rotor in Forward Flight," *NACA Report 716*, 1941.

[14]G. D. Padfield, *Helicopter Flight Dynamics*. Wiley Online Library, 2008.

[15]M. G. Ballin, "Validation of a Real-Time Engineering Simulation of the UH-60A Helicopter," *NASA TM-88360*, 1987.

[16]B. L. Stevens, F. L. Lewis, and E. N. Johnson, *Aircraft Control and Simulation: Dynamics, Controls Design, and Autonomous Systems*. John Wiley & Sons, 2015.

[17]M. B. Tischler and R. K. Remple, "Aircraft and Rotorcraft System Identification," *AIAA education series*, p. 72, 2006.

[18]E. Shinseki and J. Hudson, "Operator's Manual for UH-60A Helicopter, UH-60L Helicopter, EH-60A Helicopter," tech. rep., Department of the Army Washington DC, 1996.